ropoiesis is unclear, the repose of functionally inactivated IGF-1 in the bone marrow might resolve the problems regarding anemia in patients receiving ADT. Further studies are warranted to investigate the discordance in the GH/IGF-1 axis during ADT, as well as the influence of androgens on erythropoiesis.

Acknowledgments. The authors thank H. Yamada, M.D., for his assistance in the endocrinological data acquisition and analysis, and T. Abe, M.D., for his contribution to the hematological data analysis.

References

1. Greenspan SL, Coates P, Sereika SM, et al. Bone loss after initiation of androgen deprivation therapy in patients with prostate cancer. *J Clin Endocrinol Metab.* 2005;90:6410-6417.
2. Pinkawa M, Fischedick K, Piroth MD, et al. Prostate-specific antigen kinetics after brachytherapy or external beam radiotherapy and neoadjuvant hormonal therapy. *Urology.* 2007;69:129-133.
3. Nishiyama T, Ishizaki F, Anraku T, et al. The influence of androgen deprivation therapy on metabolism in patients with prostate cancer. *J Clin Endocrinol Metab.* 2005;90:657-660.
4. Levy ME, Perera S, van Londen GJ, et al. Physical function changes in prostate cancer patients on androgen deprivation therapy: a 2-year prospective study. *Urology.* 2008;71:735-739.
5. Alibhai SM, Rahman S, Warde PR, et al. Prevention and management of osteoporosis in men receiving androgen deprivation therapy: a survey of urologists and radiation oncologists. *Urology.* 2006; 68:126-131.
6. Nilsson-Ehle H, Jagenburg R, Landahl S, et al. Blood haemoglobin declines in the elderly: implications for reference intervals from age 70 to 88. *Eur J Haematol.* 2000;65:297-305.
7. Daughaday WH, Rotwein P. Insulin-like growth factors I and II. Peptide, messenger ribonucleic acid and gene structures, serum, and tissue concentrations. *Endocr Rev.* 1989;10:68-91.
8. Chahal HS, Drake WM. The endocrine system and ageing. *J Pathol.* 2007;211:173-180.
9. Moromisato DY, Roberts C Jr, Brasel JA, et al. Erythrocyte insulin-like growth factor-I binding in younger and older males. *Clin Endocrinol (Oxford).* 1998;48:339-345.
10. Masala A, Atzeni MM, Alagna S, et al. Growth hormone secretion in polytransfused prepubertal patients with homozygous beta-thalassemia. Effect of long-term recombinant GH (recGH) therapy. *J Endocrinol Invest.* 2003;26:623-628.
11. Vihervuori E, Virtanen M, Koistinen H, et al. Hemoglobin level is linked to growth hormone-dependent proteins in short children. *Blood.* 1996;87:2075-2081.
12. Sohmiya M, Kato Y. Effect of long-term administration of recombinant human growth hormone (rhGH) on plasma erythropoietin (EPO) and haemoglobin levels in anaemic patients with adult GH deficiency. *Clin Endocrinol (Oxford).* 2001;55:749-754.
13. Christ ER, Cummings MH, Westwood NB, et al. The importance of growth hormone in the regulation of erythropoiesis, red cell mass, and plasma volume in adults with growth hormone deficiency. *J Clin Endocrinol Metab.* 1997;82:2985-2990.
14. Isahaya E, Hara N, Nishiyama T, et al. Bone metabolic disorder in patients with prostate cancer receiving androgen deprivation therapy (ADT): impact of ADT on the growth hormone/insulin-like growth factor-1/parathyroid hormone axis. *Prostate,* in press.
15. Janssen JA, Wildhagen MF, Ito K, et al. Circulating free insulin-like growth factor (IGF)-I, total IGF-I, and IGF binding protein-3 levels do not predict the future risk to develop prostate cancer: results of a case-control study involving 201 patients within a population-based screening with a 4-year interval. *J Clin Endocrinol Metab.* 2004;89:4391-4396.
16. Miyagawa S, Kobayashi M, Konishi N, et al. Insulin and insulin-like growth factor I support the proliferation of erythroid progenitor cells in bone marrow through the sharing of receptors. *Br J Haematol.* 2000;109:555-562.
17. Kling PJ, Taing KM, Dvorak B, et al. Insulin-like growth factor-I stimulates erythropoiesis when administered enterally. *Growth Factors.* 2006;24:218-223.
18. Gutiérrez S, Mukdsi JH, Aoki A, et al. Ultrastructural immunolocalization of IGF-1 and insulin receptors in rat pituitary culture: evidence of a functional interaction between gonadotroph and lactotroph cells. *Cell Tissue Res.* 2007;327:121-132.
19. Huang YS, Rousseau K, Le Belle N, et al. Insulin-like growth factor-I stimulates gonadotrophin production from eel pituitary cells: a possible metabolic signal for induction of puberty. *J Endocrinol.* 1998;159:43-52.
20. Nelson AE, Howe CJ, Nguyen TV, et al. Erythropoietin administration does not influence the GH—IGF axis or makers of bone turnover in recreational athletes. *Clin Endocrinol (Oxford).* 2005; 63:305-309.
21. Lee P, Gelbart T, Waalen J, et al. The anemia of ageing is not associated with increased plasma hepcidin levels. *Blood Cells Mol Dis.* 2008;41:252-254.
22. Anawalt BD, Merriam GR. Neuroendocrine aging in men. Andropause and somatopause. *Endocrinol Metab Clin North Am.* 2001;30: 647-669.
23. Sommers BD, Beard CJ, D'Amico AV, et al. Somatopause: dismetabolic and bone effects. *J Endocrinol Invest.* 2005;28:36-42.
24. Hero M, Wickman S, Hanhijärvi R, et al. Pubertal upregulation of erythropoiesis in boys is determined primarily by androgen. *J Pediatr.* 2005;146:245-252.

Clin Exp Med (2010) 10:99–106
DOI 10.1007/s10238-009-0073-x

ORIGINAL ARTICLE

Structural changes in α1-adrenoceptor antagonist-treated human prostatic stroma

Tetsuya Imamura · Kenichiro Ishii · Hideki Kanda · Shigeki Arase · Yuko Yoshio · Yasuhide Hori · Norihito Soga · Hideaki Kise · Kiminobu Arima · Yoshiki Sugimura

Received: 1 June 2009 / Accepted: 22 September 2009 / Published online: 14 October 2009

Abstract α1-Adrenoceptor antagonists (α1-blockers) are currently used as first-line drugs for the treatment of benign prostatic hyperplasia (BPH). However, cases of BPH are often encountered in which the efficacy of α1-blockers decreases and switching to surgical treatment is required. One factor responsible for this resistance includes structural changes in prostatic tissue architecture following repeated oral administration of α1-blockers. Forty patients suspected of having prostate cancer, but without evidence of malignancy on prostatic biopsy were divided into two groups: an untreated group ($n = 17$) and an oral α1-blocker-treated group ($n = 23$). Twenty-one patients exhibiting resistance to oral α1-blocker therapy who underwent surgery were assigned into the surgically treated group. Each tissue sample was subjected to Masson's trichrome staining to distinguish collagen fibers from smooth muscle constituting prostatic stroma. The mean collagen fiber share was 62.2 ± 10.4% in the untreated group, 72.1 ± 9.1% in the oral α1-blocker-treated group, and 72.2 ± 15.7% in the surgically treated group. Focusing on cases exhibiting high-collagen fiber share (70% or more), the distribution in each of the two α1-blocker-treated groups (16 of the 23 cases from the oral α1-blocker-treated group and 10 of the 21 cases from the surgically treated group) differed significantly from that in the untreated group (2 of the 17 cases). Our findings suggest that the accumulation of collagen fibers in prostatic stroma could be one of the factors responsible for α1-blocker treatment.

Keywords α1-Adrenoceptor antagonist · Benign prostatic hyperplasia · Prostatic tissue architecture · Collagen fiber · Morphometrical analysis

Introduction

Benign prostatic hyperplasia (BPH) is frequently observed in middle-aged and elderly males; its prevalence is only 8% in the 30s, but more than 70% in the 60s [1]. Its major manifestations are lower urinary tract symptoms. Because it is benign, severe complications are rare. However, from the standpoint of preserving the quality of life (QOL), it is essential to alleviate symptoms when dealing with patients with BPH. Regarding the natural history of BPH, Berry et al. [1] reported that prostate weight increases sharply as male hormone secretion increases before adolescence, although the rate of increase in it becomes much smaller after the age of 30. However, prostate weight begins to increase again over the age 60, with a sharp increase in the 70s. In an analysis of Japanese cases reported by Fujikawa et al. [2], prostate weight tended to increase sharply from birth to age 20s and then increased gradually, with no sharp increase after age 60. These two reports suggest that prostate weight is lower in Japanese than in Western individuals and that prostate weight gain is less in the Japanese.

According to the hypothesis proposed by McNeal [3], BPH nodules are the result of reappearance of embryonic ductal morphogenesis, and BPH develops through a change

T. Imamura and K. Ishii contributed equally to this work.

T. Imamura · K. Ishii · H. Kanda · S. Arase · Y. Yoshio · Y. Hori · N. Soga · H. Kise · K. Arima · Y. Sugimura (✉)
Department of Nephro-Urologic Surgery and Andrology, Mie University Graduate School of Medicine, 2-174 Edobashi, Tsu, Mie 514-8507, Japan
e-mail: sugimura@clin.medic.mie-u.ac.jp

in stromal differentiation into fetal phenotype. Norman et al. [4] suggested that in mice, the fetal stroma reacts with post-developmental prostate epithelium, resulting in the formation of new prostate tissue. Their report favors the hypothesis of McNeal [3] and suggests that various growth factors, cytokines, and other agents involved in interactions between stroma and epithelial cells are related to the onset of BPH.

At present, BPH is treated by drug therapy, surgery (primarily transurethral resection of the prostate; TURP) and low-invasive therapy using lasers, stents, and other means. α1-adrenoceptor antagonists (α1-blockers) are often used as first-line drugs [5]. Even at present, 15 years after clinical use of them was begun, α1-blockers are considered useful in the treatment of BPH. They suppress functional contraction of prostatic smooth muscle by blocking the signal from the α1-adrenoceptors distributed in this muscle. They thereby reduce urethral resistance and improve urination. Representative α1-blockers used in Japan include tamsulosin hydrochloride and silodosin, which exert selective effects on α1a receptors, and naftopidil, which has relatively high affinity for α1d receptors.

In routine urological practice, cases of BPH in which responses to α1-blockers decrease are often noted, necessitating surgical treatment. In an analysis of clinical parameters aimed at identifying factors responsible for the development of resistance to drugs, Ichioka et al. [6] reported that the resistance of BPH to drugs is related to pre-treatment international prostate symptom score (I-PSS), and Masumori et al. [7] reported the association of this resistance with prostate weight. Shapiro et al. [8] found that the percentage of prostatic stroma occupied by smooth muscle differed between responders and non-responders to drugs. More recently, Justulin et al. [9] reported reduction in smooth muscle and accumulation of collagen in rat prostate glands following the treatment with doxazosin suggesting that structural changes can also occur in α1-blocker-treated human prostate gland. Structural changes in prostatic tissue architecture thus also appear to be associated with the development of resistance of BPH to drug therapy.

Based on the view that oral α1-blocker treatment can alter the prostatic tissue architecture and that this is one of the factors responsible for the development of resistance of BPH to drugs, we analyzed the composition of stroma in human prostate. Biopsied prostate tissue and surgically resected prostate tissue were subjected to Masson's trichrome staining to distinguish collagen fibers from smooth muscle constituting the prostatic stroma and to explore differences in tissue architecture between patients given no α1-blocker treatment and those orally treated with α1-blockers.

Materials and methods

Patient background

Forty patients suspected of having prostate cancer based on the elevated serum prostate-specific antigen (PSA) (more than 4 ng/mL), but without sign of malignancy on prostatic biopsy were divided into two groups: an untreated group ($n = 17$) and an oral α1-blocker-treated group ($n = 23$). Twenty-one patients exhibiting resistance to oral α1-blocker therapy who underwent surgery were assigned to a third group (the surgically treated group). Prostate volume was measured on transrectal ultrasonography. In this study, over 20.0 mL of prostate was considered BPH tissue. The α1-blockers used in the oral α1-blocker-treated group were tamsulosin (20 cases) and naftopidil (3 cases), whereas those used in the surgically treated group were tamsulosin (17 cases), naftopidil (3 cases), and uradipil (1 case). Patients orally treated with α1-blockers for 12 weeks or longer were considered orally treated.

Evaluation of clinical symptoms

In each group, clinical symptoms were evaluated with the international prostate symptom score (I-PSS) and quality of life (QOL) index [10]. In evaluation with I-PSS, the total of the scores for the following seven symptoms was calculated as the total I-PSS for each patient: (1) sensation of residual urine, (2) pollakiuria, (3) interrupted urine stream, (4) urinary urgency, (5) forceless urinary stream, (6) abdominal straining during micturition, and (7) nocturnal pollakiuria. Evaluation with the QOL index involved a question ("To what extent will you be satisfied if your current status of urination persists from now on?") for each patient and assessment of the response (degree of satisfaction) on a 7-category scale: 0 delighted, 1 pleased, 2 mostly satisfied, 3 mixed about equally satisfied and dissatisfied, 4 mostly dissatisfied, 5 unhappy and 6 terrible.

Evaluation with both the I-PSS and QOL index was possible in all of the 17 patients from the untreated group, 21 of the 23 patients from the oral α1-blocker-treated group, and all of the 21 patients from the surgically treated group. For the untreated group, evaluation with the I-PSS and QOL index was carried out only during the first visit. For the oral α1-blocker-treated group and the surgically treated group, the evaluation with the I-PSS and QOL index was carried out before the start of oral drug therapy and 12 weeks after the start of oral drug therapy.

Tissue processing

Each biopsied tissue specimen was immediately fixed in 10% neutral formalin buffer. Each surgical specimen (of

the transitional area of the prostate) was immersed in RPMI-1640 tissue culture medium (Sigma–Aldrich, St Louis, MO) and stored at 4°C, and fixed in formalin within 2 h after resection. Paraffin blocks were then prepared and sliced at a thickness of 4 μm with a Leica RM2125 rotary microtome (Leica Microsystems, Wetzlar, Germany).

Masson's trichrome staining

Deparaffinized sections were exposed to a first mordant solution (10% potassium dichromate combined with an equal amount of 10% acetate dichromate; Muto Pure Chemicals Co., Ltd, Tokyo, Japan) for 10 min. After washing, the sections were exposed to iron hematoxylin solution (Weigert's iron hematoxylin solution 1 combined with an equal amount of Weigert's iron hematoxylin solution 2; Muto Pure Chemicals Co., Ltd, Tokyo, Japan) for 10 min to induce nuclear staining. After the sections had been washed with flowing water, they were exposed to a second mordant solution (2.5% phosphotungstic acid combined with an equal amount of 2.5% phosphomolybdic acid; Muto Pure Chemicals Co., Ltd, Tokyo, Japan) for 45 s. They were then exposed to 0.75% orange G solution (Muto Pure Chemicals Co., Ltd, Tokyo, Japan) for 1 min. After washing with a 1% aqueous solution of acetic acid, sections were exposed to Masson's dye solution (a mixture of ponceau de xylidine, acid fuchsin, and azophloxin; Muto Pure Chemicals Co., Ltd, Tokyo, Japan) for 10 min to stain cytoplasm red. After washing with 1% aqueous solution of acetic acid, sections were exposed to 2.5% phosphotungstic acid solution (Muto Pure Chemicals Co., Ltd, Tokyo, Japan) for 10 min. After washing with 1% aqueous solution of acetic acid, they were exposed to aniline blue (Muto Pure Chemicals Co., Ltd, Tokyo, Japan) for 5 min to induce blue staining of collagen fibers. Staining was carried out at room temperature.

Image analysis

Images were taken of the biopsied tissue specimens (of the transitional area of the prostate). Each specimen was after Masson's trichrome staining photographed with a microscopic digital camera (DP 70, Olympus Corporation, Tokyo, Japan) combined with a system biomicroscope (BX50, Olympus Corporation, Tokyo, Japan) at a magnification of 200×. The images were fed into a computer. On each section, photography was performed at two sites at maximum. In total, photography of five visual fields of transitional areas was performed. In addition, for each surgical specimen, photography was performed at two sites of the same section at maximum (ten visual fields in total). Using the Win ROOF ver. 5.7 image analysis program (Mitani, Fukui, Japan), the gland cavities were removed from each image, and the area of prostatic stroma occupied by collagen fibers and that occupied by smooth muscle were measured, and their percentages were calculated (Fig. 1a–d). Referring to the report of Shapiro et al. [11] that the mean percentages of prostatic stroma occupied by collagen fibers and smooth muscle were 71 and 29%, respectively, in patients with BPH, we divided the patients into a high-collagen fiber share group and a low-collagen fiber share group on the basis of the percentage of prostatic stroma occupied by collagen fibers (cut-off level 70%).

Statistical analysis

The results are the mean ± SD. Student's t test was used for comparisons of collagen fiber share. The Mann–Whitney's U test was employed for intergroup comparisons of the I-PSS and QOL index data collected to evaluate clinical symptoms from the three groups. The Wilcoxon-signed rank test was used for the analysis of changes in I-PSS and QOL index scores at 12 weeks after the start of oral drug therapy from pretreatment levels within the same group. The χ^2 test was employed for comparisons of frequencies and percentages among the three groups.

Results

The study involved three groups of patients. Forty patients who underwent prostate biopsy were divided into an untreated group ($n = 17$) and an oral α1-blocker-treated group ($n = 23$). The third group was composed of 21 patients who underwent surgery after exhibiting resistance to oral α1-blocker therapy. There was no marked difference in age or serum PSA level between any two of the three groups (Table 1). Prostate weight was significantly larger in the two groups receiving oral α1-blocker treatment than in the untreated group ($P < 0.05$) (Table 1).

In evaluation of clinical symptoms, the total I-PSS and QOL index during the first visit were significantly higher in the oral α1-blocker-treated group and the surgically treated group than in the untreated group ($P < 0.01$) (Table 2). In the oral α1-blocker-treated group, these scores were significantly decreased by 12 weeks of treatment with α1-blockers, i.e. the disturbance of lower urinary tract passage was improved by α1-blocker administration. In contrast, these scores in the surgically treated group even after α1-blocker administration were still higher than in the untreated group ($P < 0.01$), i.e. it was necessary to switch from drug therapy to surgery.

Masson's trichrome staining was carried out for these three groups to distinguish collagen fibers from smooth muscle constituting the prostatic stroma. In examples of staining of surgically resected transitional area of the

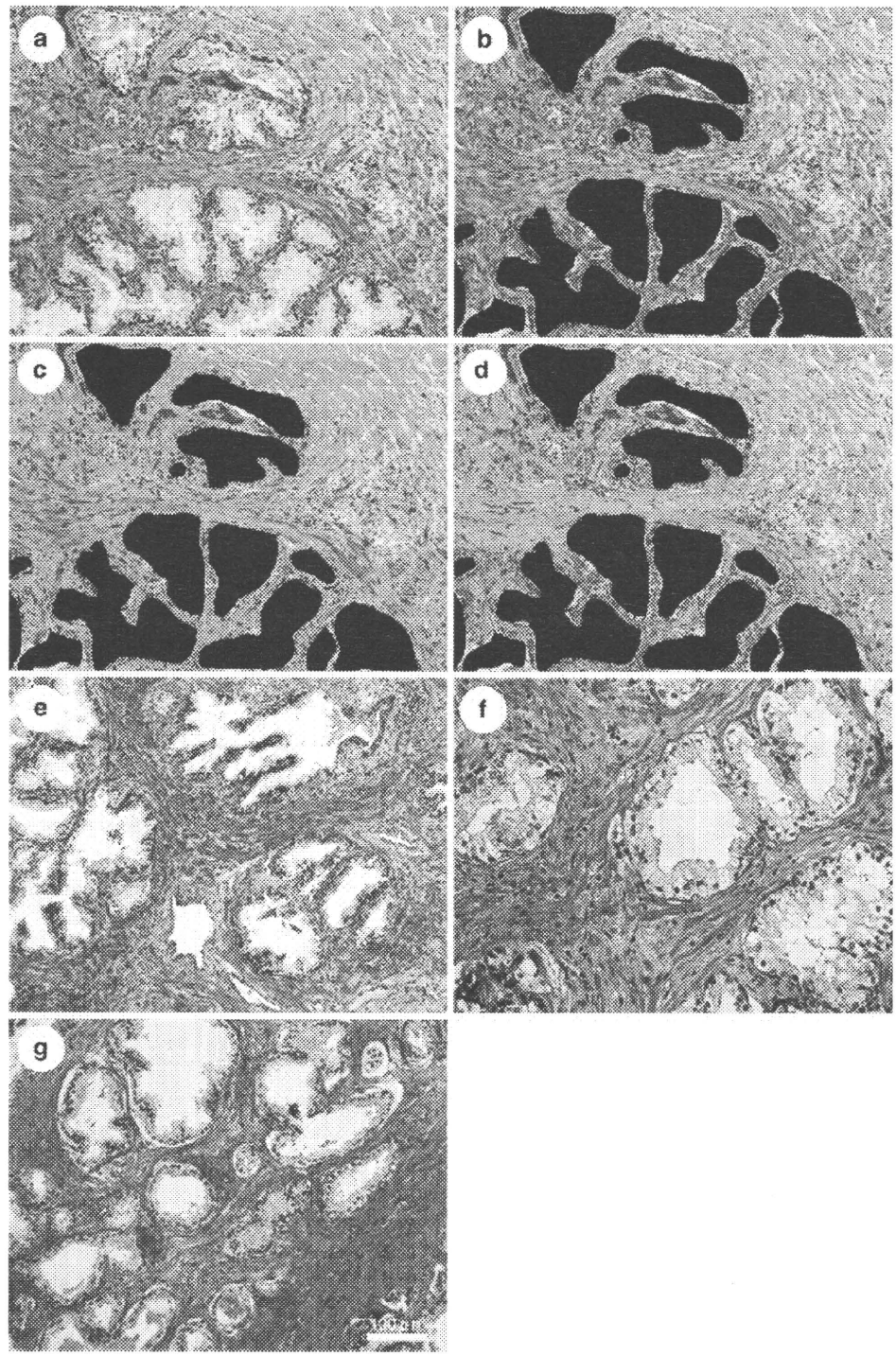

Fig. 1 Quantitative image analysis of collagen fibers in human prostatic stroma. Masson's trichrome staining was performed on all specimens. The image was captured into a computer **a**, and then the gland cavities were removed **b**. The area of prostatic stroma occupied by collagen fibers **c** and that occupied by smooth muscle **d** were measured, and their percentages were calculated in each image. Representative Masson's trichrome-stained human prostate tissue with BPH is illustrated (**e**, **f**, and **g**). Share of collagen fibers were as follows: **e**. 43.0%, **f**. 71.0%, **g**. 94.0% (×200)

prostate, percentages of collagen fibers were as follows: e. 43.0%, f. 71.0%, g. 94.0% (Fig. 1). A higher share of collagen fibers is reflected in an increase in blue-stained area.

When collagen fiber share and distribution of frequency was compared among the three groups, the number of cases with high-collagen fiber share (70% or more) in both oral α1-blocker-treated group and surgically treated group was greater than that in the untreated group (Fig. 2). In the untreated group (Fig. 2a, d, g), collagen fiber share showed a moderate positive correlation with age ($y = 0.627x + 21.274$, $r = 0.552$), prostate volume ($y = 0.294x + 51.083$, $r = 0.561$), and serum PSA ($y = 0.688x + 55.351$, $r = 0.415$). However, a weak positive or negative correlation between collagen fiber share and other factors was observed in each of the two

Table 1 Characteristics of patient

	Biopsy		Surgically treated
	Untreated	α1-Blocker treated	α1-Blocker treated
Patient (*n*)	17	23	21
Age (years) (range)	65.2 ± 9.2 (48–81)	70.9 ± 6.6 (60–80)	69.1 ± 6.1 (61–84)
Prostate volume (mL) (range)	37.8 ± 19.8 (20.0–86.8)	52.6 ± 24.3* (20.0–105.2)	56.0 ± 30.7* (20.0–133.0)
PSA (ng/mL) (range)	9.9 ± 6.3 (3.6–24.2)	7.5 ± 3.0 (4.2–14.4)	8.0 ± 4.4 (1.1–17.2)
Medication		Tamsulosin 20	Tamsulosin 17
		Naftopidil 3	Naftopidil 3
			Uradipil 1

* $P < 0.05$ versus untreated

Table 2 Change from baseline to 12 weeks of treatment in I-PSS and QOL index for overall patients treated with α1-blocker and untreated

	Treatment	I-PSS		QOL index	
		Before	After	Before	After
Biopsy	Untreated (range) $n = 17$	7.7 ± 8.4 (0–29)		2.2 ± 1.3 (1–6)	
Biopsy	α1-Blocker treated (range) $n = 21$	16.4 ± 5.1* (9–26)	9.8 ± 4.5‡ (4–23)	4.7 ± 0.6* (4–6)	2.9 ± 1.0‡ (2–5)
Surgically treated	α1-Blocker treated (range) $n = 21$	21.1 ± 5.9*† (7–32)	17.7 ± 7.1*‡ (4–32)	4.8 ± 0.5*(4–6)	4.0 ± 1.0*‡ (2–6)

* $P < 0.01$ versus untreated group evaluated by Mann–Whitney's *U* test

† $P < 0.05$ versus oral α1-blocker-treated group before treatment evaluated by Mann–Whitney's *U* test

‡ $P < 0.01$ versus before treatment in each group evaluated by Wilcoxon-signed rank test

α1-blocker-treated groups (the oral α1-blocker treatment group and the surgically treated group). The collagen fiber share was 62.2 ± 10.4% (48.4–93.8) in the untreated group, 72.1 ± 9.1% (51.0–89.3) in the oral α1-blocker-treated group, and 72.2 ± 15.7% (47.1–99.3) in the surgically treated group (Table 3). The mean collagen fiber share in each of the two α1-blocker-treated groups differed significantly from that in the untreated group ($P < 0.05$) (Table 3). Among the cases in which collagen fiber share was low (less than 70%), there was no significant difference in mean collagen fiber share between any two of the three groups. However, when the distribution of collagen fiber share was examined for cases exhibiting high-collagen fiber share (70% or more), the distribution in each of the two α1-blocker-treated groups (16 of the 23 cases from the oral α1-blocker-treated group and 10 of the 21 cases from the surgically treated group) differed significantly from that in the untreated group (2 of the 17 cases) ($P < 0.05$) (Table 3).

Discussion

The present study using clinical specimens found that patients orally treated with α1-blockers often exhibit high-collagen fiber share in the prostatic stroma. Our findings also suggested that patients who had undergone surgery, after the manifestation of resistance to drug therapy were more likely to exhibit high-collagen fiber share in the prostatic stroma. However, high-collagen fiber share was not always observed in patients orally treated with α1-blockers indicating that the effects of oral α1-blocker treatment on the tissue architecture of prostatic stroma vary among patients.

It is known that the stromal nodules associated with BPH are composed of immature mesenchymal cells, fibroblasts, myofibroblasts, and smooth muscle cells [12]. In a study using prostatic smooth muscle cells, Smith et al. [13] found that contractility of smooth muscle cells decreased following inhibition of adrenergic receptor signaling by α1-blockers. Their finding suggests that α1-blockers induce dedifferentiation of smooth muscle into fibroblasts and myofibroblasts, and may thus induce alteration of tissue architecture. More recently, Justulin et al. [9] reported that when rats were given repeated doses of doxazosin, they exhibited collagen fiber accumulation in prostatic stroma and reduction in smooth muscle. On the basis of this finding, they suggested the possibility that continued oral treatment with doxazosin would alter prostatic tissue architecture and reduce the efficacy of α1-blockers [9]. These views were endorsed by the findings of our study, in which treatment with α1-blockers resulted in alteration of prostatic tissue architecture. However, the mechanisms responsible for such changes have not yet

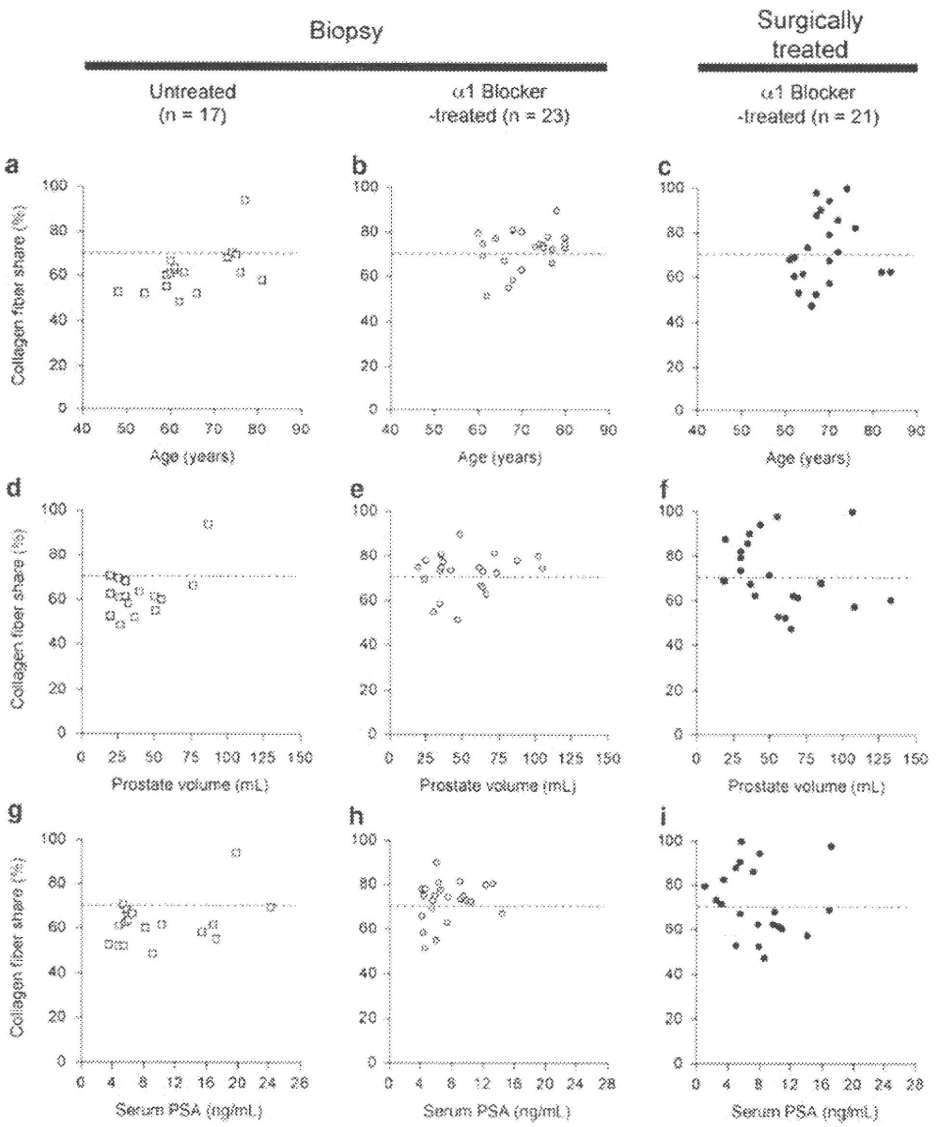

Fig. 2 Collagen fiber share in relation to the presence/absence of oral α1-blocker treatment. In comparison with age (**a–c**), prostate volume (**d–f**), and serum PSA (**g–i**), the distribution of collagen fiber share in individual cases is graphically represented for each of the three groups: the untreated group (17 patients receiving no oral α1-blocker after prostate biopsy; **a**, **d**, and **g**), the oral α1-blocker-treated group (23 patients orally treated with α1-blockers following biopsy; **b**, **e**, and **h**), and the surgically treated group (21 patients who underwent surgery after exhibiting resistance to oral α1-blocker treatment; **c**, **f**, and **i**)

Table 3 Comparison of fibrotic area in human prostate tissues

	Biopsy		Surgically treated
	Untreated	α1-Blocker treated	α1-Blocker treated
Total Pt			
Percentage of fibrotic area	62.2 ± 10.4	72.1 ± 9.1**	72.2 ± 15.7*
Range	(48.4–93.8)	(51.0–89.3)	(47.1–99.3)
Number	17	23	21
Group of ≥70.0%			
Percentage of fibrotic area	82.1 ± 16.6	76.9 ± 4.5	85.8 ± 9.7
Number (%)	2 (11.8)	16 (69.6)††	10 (47.6)†
Group of <70.0%			
Percentage of fibrotic area	59.5 ± 6.3	61.0 ± 6.6	59.7 ± 7.0
Number (%)	15 (88.2)	7 (30.4)	11 (52.4)

* $P < 0.05$

** $P < 0.01$ versus untreated evaluated by t test

† $P < 0.05$

†† $P < 0.001$ versus untreated evaluated by χ^2 test

been elucidated. Justulin et al. [9] referred to transforming growth factor-β (TGF-β) as an intracellular transmitter possibly involved in such changes. TGF-β is a cytokine with diverse functions. In the extracellular matrix (ECM), it is known that fibroblasts, osteoblasts, odontoblasts, and other types of cells induce the expression of COL1A1 and COL1A2 (genes encoding type I collagen) in the presence of TGF-β, resulting in the stimulation of type I collagen formation [14].

With regard to the size of prostate, Ishigooka et al. [15] reported a correlation between prostate volume and increase in fibrous tissue in a histological examination of surgical specimens collected by TURP, suggesting that fibrous tissue plays an important role in prostatic hyperplasia. Ichiyanagi et al. [16] performed a histological examination of specimens from TURP and found that the share of stroma and that of gland cavities in the prostate differed little between patients with and without disturbance of lower urinary tract passage, while the share of smooth muscle in prostatic stroma was significantly lower in patients with disturbance of lower urinary tract passage. In the present study, mean percentage of collagen fibers was higher in the two groups of patients who received oral α1-blocker treatment (the oral α1-blocker-treated group and the surgically treated group), while the high I-PSS and QOL index, indices of disturbance of lower urinary tract passage, were not observed in the oral α1-blocker-treated group. Thus, our results suggest that high accumulation of collagen fibers in prostatic stroma following the loss of smooth muscle may not be associated with the clinical symptoms.

In clinical usage, α1-blockers are known to suppress the contraction of prostatic smooth muscle and thus alleviate urinary symptoms. Shapiro et al. [8] reported that the share of smooth muscle in prostatic stroma was 38% higher in patients responding to α1-blockers than in patients failing to respond to α1-blockers. It is plausible to suggest, then, that decrease in smooth muscle may suppress contraction and thus alleviate dysuria. As shown in the above-cited studies by Ishigooka et al. [15] and Ichiyanagi et al. [16], lower urinary tract obstruction and prostatic hyperplasia are associated with an increase in fibrous tissue, i.e., a decrease in smooth muscle tissue. Thus, it appears likely that the presence of smooth muscle allows muscle tonus to be preserved. Therefore, these findings of the present and previous studies suggest that the share of smooth muscle in prostatic stroma is an important factor determining response to α1-blockers. The present study revealed the presence of many cases with high accumulation of collagen fibers in prostatic stroma following the loss of smooth muscle in the groups that received oral α1-blocker treatment, while there were also patients in whom collagen fiber share was not high despite the oral α1-blocker treatment. These findings suggest that effects of the histological architecture of prostatic stroma (as related to the balance between collagen fibers and smooth muscle) on the pharmacological efficacy of α1-blockers may vary among individual patients.

The analysis of our findings suggests that patients exhibiting high-collagen fiber share in the oral α1-blocker-treated group are likely to exhibit decreased response to α1-blockers, necessitating switching from drug therapy to surgery. However, high-collagen fiber share was not observed in all of the patients for whom drug therapy was switched to surgery, and there were some cases in which other factors forced switching from drug therapy to surgery, e.g., age, prostate volume, and bladder function. Thus, a high-collagen fiber share in prostatic stroma may not be considered the major factors responsible for development of resistance to α1-blocker therapy and necessitating switching to surgery. Further investigation is necessary to determine the molecular mechanisms by which resistance to oral α1-blocker treatment has developed in individual patients.

In conclusion, α1-blockers are currently used as first-line drugs for the treatment of BPH. They are highly efficacious in alleviating lower urinary tract symptoms, and are, therefore, frequently used clinically. However, some patients develop resistance to this class of drug after prolonged oral use. The findings of the present study suggest that the accumulation of collagen fibers in prostatic stroma following the loss of smooth muscle could be one of the factors responsible for α1-blocker treatment. Our data also may indicate that the effects of oral α1-blockers on the tissue architecture of the prostatic stroma vary among patients.

Acknowledgments This study was financially supported by Grants-in-Aid from the Ministry of Education for Science and Culture of Japan (Nos. 18591748, 19591841, and 19659412). The authors thank the physicians working at Suzuka Chuou General Hospital, Mie Chuou Medical Center, Saiseikai Matsusaka General Hospital, Mie Prefectural General Medical Center, and Takeuchi Hospital, who are members of the Mie Clinical Urologic Research Entry (M-CURE) and supplied tissue specimens for this study. The authors also thank Mrs. Hiroko Nishii for her support in histopathological analysis.

Conflict of interest statement The authors declare that they have no conflict of interest related to the publication of this manuscript.

References

1. Berry SJ, Coffey DS, Walsh PC, Ewing LL (1984) The development of human benign prostatic hyperplasia with age. J Urol 132:474–479
2. Fujikawa S, Matsuura H, Kanai M, Fumino M, Ishii K, Arima K, Shiraishi T, Sugimura Y (2005) Natural history of human prostate gland: morphometric and histopathological analysis of Japanese men. Prostate 65:355–364

3. McNeal JE (1978) Origin and evolution of benign prostatic enlargement. Invest Urol 15:340–345
4. Norman JT, Cunha GR, Sugimura Y (1986) The induction of new ductal growth in adult prostatic epithelium in response to an embryonic prostatic inductor. Prostate 8:209–220
5. Djavan B, Marberger M (1999) A meta-analysis on the efficacy and tolerability of alpha1-adrenoceptor antagonists in patients with lower urinary tract symptoms suggestive of benign prostatic obstruction. Eur Urol 36:1–13
6. Ichioka K, Ohara H, Terada N, Matsui Y, Yoshimura K, Terai A, Arai Y (2004) Long-term treatment outcome of tamsulosin for benign prostatic hyperplasia. Int J Urol 11:870–875
7. Masumori N, Hashimoto J, Itoh N, Tsukamoto T, Group TS (2007) Short-term efficacy and long-term compliance/treatment failure of the alpha1 blocker naftopidil for patients with lower urinary tract symptoms suggestive of benign prostatic hyperplasia. Scand J Urol Nephrol 41:422–429
8. Shapiro E, Hartanto V, Lepor H (1992) The response to alpha blockade in benign prostatic hyperplasia is related to the percent area density of prostate smooth muscle. Prostate 21:297–307
9. Justulin LA Jr, Delella FK, Felisbino SL (2008) Doxazosin reduces cell proliferation and increases collagen fibers in rat prostatic lobes. Cell Tissue Res 332:171–183
10. Barry MJ, Williford WO, Chang Y, Machi M, Jones KM, Walker-Corkery E, Lepor H (1995) Benign prostatic hyperplasia specific health status measures in clinical research: how much change in the American Urological Association symptom index and the benign prostatic hyperplasia impact index is perceptible to patients? J Urol 154:1770–1774
11. Shapiro E, Hartanto V, Lepor H (1992) Quantifying the smooth muscle content of the prostate using double-immunoenzymatic staining and color assisted image analysis. J Urol 147:1167–1170
12. Bierhoff E, Vogel J, Benz M, Giefer T, Wernert N, Pfeifer U (1996) Stromal nodules in benign prostatic hyperplasia. Eur Urol 29:345–354
13. Smith P, Rhodes NP, Ke Y, Foster CS (1999) Influence of the alpha1-adrenergic antagonist, doxazosin, on noradrenaline-induced modulation of cytoskeletal proteins in cultured hyperplastic prostatic stromal cells. Prostate 38:216–227
14. Verrecchia F, Mauviel A (2007) Transforming growth factor-beta and fibrosis. World J Gastroenterol 13:3056–3062
15. Ishigooka M, Hayami S, Hashimoto T, Suzuki Y, Katoh T, Nakada T (1996) Relative and total volume of histological components in benign prostatic hyperplasia: relationships between histological components and clinical findings. Prostate 29:77–82
16. Ichiyanagi O, Sasagawa I, Ishigooka M, Suzuki Y, Nakada T (2000) Morphometric analysis of symptomatic benign prostatic hyperplasia with and without bladder outlet obstruction. Urol Res 28:29–32

DOI:10.1158/1078-0432.CCR-06-2225

Epigenetic Modifications of *RASSF1A* Gene through Chromatin Remodeling in Prostate Cancer

Ken Kawamoto,[1] Steven T. Okino,[1] Robert F. Place,[1] Shinji Urakami,[1] Hiroshi Hirata,[1] Nobuyuki Kikuno,[1,2] Toshifumi Kawakami,[1] Yuichiro Tanaka,[1] Deepa Pookot,[1] Zhong Chen,[1] Shahana Majid,[1] Hideki Enokida,[3] Masayuki Nakagawa,[3] and Rajvir Dahiya[1]

Abstract

Purpose: The RAS-association domain family 1, isoform A (*RASSF1A*) gene is shown to be inactivated in prostate cancers. However, the molecular mechanism of silencing of the *RASSF1A* gene is not fully understood. The present study was designed to investigate the mechanisms of inactivation of the *RASSF1A* gene through the analysis of CpG methylation and histone acetylation and H3 methylation associated with the *RASSF1A* promoter region.

Experimental Design: Methylation status of the *RASSF1A* gene was analyzed in 131 samples of prostate cancer, 65 samples of benign prostate hypertrophy (BPH), and human prostate cell lines using methylation-specific PCR. Histone acetylation (acetyl-H3, acetyl-H4) and H3 methylation (dimethyl-H3-K4, dimethyl-H3-K9) status associated with the promoter region in prostate cells were analyzed by chromatin immunoprecipitation (ChIP) assay.

Results: Aberrant methylation was detected in 97 (74.0%) prostate cancer samples and 12 (18.5%) BPH samples. The methylation frequency of *RASSF1A* showed a significant increase with high Gleason sum and high stage. The ChIP assays showed enhancement of histone acetylation and dimethyl-H3-K4 methylation on the unmethylated *RASSF1A* promoter. TSA alone was unable to alter key components of the histone code. However, after 5-aza-2′-deoxy-cytidine treatment, there was a complete reversal of the histone components in the hypermethylated promoter. Levels of acetyl-H3, acetyl-H4, and dimethyl-H3-K4 became more enriched, whereas H3K9me2 levels were severely depleted.

Conclusions: This is the first report suggesting that reduced histone acetylation or H3K4me2 methylation and increased dimethyl-H3-K9 methylation play a critical role in the maintenance of promoter DNA methylation–associated *RASSF1A* gene silencing in prostate cancer.

Prostate cancer is the most commonly diagnosed malignancy and the second leading cause of cancer-related deaths among men in the United States and Europe (1). The incidence of prostate cancer increases with aging (2). Once a tumor has metastasized, the long-term prognosis is poor because no curative therapy is available. Cancer development and metastasis are multistep processes that, among others, involve the inactivation of tumor suppressor genes. When normal expression levels of these growth-inhibitory proteins are suppressed, uncontrolled cell cycling and growth can result. Identifying such specific molecular changes may contribute to improved diagnosis, clinical management, and outcome prediction of newly diagnosed prostate cancers (3).

Silencing of cancer-associated genes by hypermethylation of CpG islands within the promoter and/or 5′ regions is a common feature of human cancer and is often associated with partial or complete transcriptional block (4). This epigenetic alteration provides an alternative pathway to gene silencing in addition to gene mutation or deletion. Moreover, the finding of promoter methylation of several genes in small biopsies and bodily fluids of cancer patients has proven to be useful as a molecular tool for cancer detection (5, 6).

The RAS-association domain family 1 has seven different isoforms that are produced by alternative splicing and transcription from two different promoters with CpG islands (7, 8). The RAS-association domain family 1, isoform A (*RASSF1A*) gene is a tumor suppressor gene in the RAS pathway that can regulate proliferation, induce apoptosis, and bind to and stabilize microtubules (9). Inactivation of *RASSF1A* is frequently observed in a number of solid tumors and epithelial cancers, including prostate cancer (3, 10–17).

Authors' Affiliations: [1]Department of Urology, Veterans Affairs Medical Center and University of California School of Medicine, San Francisco, California; [2]Department of Urology, Shimane University, Faculty of Medicine, Izumo 693-8501, Japan; and [3]Department of Urology, Graduate School of Medical and Dental Sciences, Kagoshima University, Kagoshima 890-8520, Japan

Received 9/6/06; revised 2/2/07; accepted 2/16/07.

Grant support: NIH grants RO1CA101844, RO1CA111470, RO1CA108612, RO1AG21418, and T32DK07790, VA Merit Review and Research and Engineering Apprenticeship Program grants.

The costs of publication of this article were defrayed in part by the payment of page charges. This article must therefore be hereby marked *advertisement* in accordance with 18 U.S.C. Section 1734 solely to indicate this fact.

Requests for reprints: Rajvir Dahiya, Urology Research Center (112F), Veterans Affairs Medical Center and University of California School of Medicine, San Francisco, 4150 Clement Street, San Francisco, CA 94121. Phone: 415-750-6964; E-mail: rdahiya@urology.ucsf.edu.

doi:10.1158/1078-0432.CCR-06-2225

DOI:10.1158/1078-0432.CCR-06-2225

In the present study, we investigated the chromatin changes involved in the inactivation of the *RASSF1A* gene in prostate cancer samples through the analysis of CpG methylation in the promoter regions, histone acetylation (acetyl-H3, acetyl-H4), dimethyl-H3-K4 (H3K4me2), and dimethyl-H3-K9 (H3K9me2) methylation associated with the *RASSF1A* promoter region.

Materials and Methods

Clinical samples. A total of 131 newly diagnosed prostate cancer tissues from radical prostatectomy and 65 pathologically proven benign prostate hypertrophy (BPH) samples from transurethral resection (TUR-P). The pathologic background of the prostate cancer patients included Gleason sum (GS) <7 (75 cases) and GS ≥7 (56 cases); pT2 (85 cases), pT3 (44 cases), and pT4 (2 cases); and preoperative serum PSA <4.0 (18 cases), PSA 4.0-10.0 (63 cases), and PSA >10.0 (50 cases). The median follow-up time was 35.5 months, with a range from 0.7 to 91.4 months. Serum PSA levels after radical prostatectomy was used as a surrogate end point, with a level ≥0.2 ng/mL designated as PSA failure. The median age of prostate cancer and BPH patients was 70 years (49-80 years) and 75 years (54-87 years), respectively. The pathologic findings of prostate cancer samples were decided by the general rule for Clinical and Pathological Studies on Prostate Cancer by the Japanese Urological Association and the Japanese Society of Pathology (18). The routine strategy to diagnose prostate cancer included serum PSA level, transrectal ultrasonography, color Doppler ultrasonography, and MRI, which allowed accurate localization of prostate cancer before radical prostatectomy (19). Each tissue sample was fixed in 10% buffered formalin (pH 7.0) and embedded in paraffin wax. For histologic evaluation, 5-μm-thick sections were used for H&E staining. All of the samples were microscopically dissected and analyzed for methylation (20). In BPH samples, high-grade prostate intraepithelial neoplasia and cancer were ruled out by microscopic analysis.

Cell lines. RWPE-1 and PWR-1E, a nontumorigenic human prostatic epithelial cell line, and the human prostate cancer cell lines LNCaP and PC3 were obtained from the American Type Culture Collection. RWPE-1 and PWR-1E cells were maintained in keratinocyte serum-free medium (Life Technologies) supplemented with 50 μg/mL bovine pituitary extract, 5% L-glutamine, and 5 ng/mL epidermal growth factor. Both prostate cancer cell lines were maintained in RPMI 1640 with L-glutamine and sodium pyruvate. The cells were maintained in a humidified incubator (5% CO_2) at 37°C.

Nucleic acid extraction. Genomic DNA was extracted from cell lines, prostate cancer, and control prostate samples using a QIAamp DNA Mini Kit (Qiagen) after microdissection (20). The concentrations of DNA and RNA were determined spectrophotometrically, and their integrity was assessed by gel electrophoresis.

Methylation analysis. Genomic DNA from all prostate samples (100 ng) was subjected to sodium bisulfite modification using a CpGenome DNA Modification Kit (Intergen Co.). The methylation status of the promoter region of *RASSF1A* was analyzed by methylation-specific PCR (MSP) as described previously (21). The first universal primer set (PAN) covers no CpG sites in either the forward or reverse primer and amplifies a DNA fragment of the promoter region containing a number of CpG sites. Then, a second round of nested MSP or unmethylation-specific PCR (USP) was done using the universal PCR products as templates. Referring to a previous report (22), primer sequences were designed for MSP and USP. The primer sequences and PCR conditions are shown in Table 1. For semiquantitative analysis, a preliminary suitable number of PCR cycles for each MSP and USP were carried out to determine the linear range of the reaction. In each assay, the absence of DNA template served as negative control. CpGenome Universal Methylated DNA (Intergen) was used as a positive control for methylated alleles. The obtained MSP and USP products were analyzed by electrophoresis in 3% agarose gels and stained with ethidium bromide.

Bisulfite DNA sequencing. Bisulfite-modified DNA was amplified using a pair of universal primers. Direct bisulfite DNA sequencing of the PCR products using either forward universal primer or reverse primer was done according to the manufacturer's instructions (Applied Biosystems).

5′-aza-2-deoxycytidine and TSA treatment. Cells were treated with the DNA methyltransferase inhibitor 5-aza-2′-deoxy-cytidine (5-aza-dC; Sigma-Aldrich) at 5 μmol/L for 48 h and/or the histone deacetylase (HDAC) inhibitor trichostatin A (TSA, Upstate Biotechnology) at 300 nmol/L for 24 h. The genomic DNA and total RNA were extracted from the cell lines before and after drug treatment and were used for MSP and reverse transcription-PCR (RT-PCR; TITANIUM One-Step RT-PCR kit, BD Biosciences). The primer sequences (22) and PCR conditions are shown in Table 1.

Chromatin immunoprecipitation assay. Chromatin immunoprecipitation (ChIP) assays were done on cell line DNA using a EZ ChIP (Upstate Biotechnology) and followed the manufacturer's protocols with some modifications. Formaldehyde was added to the cells in a culture dish to a final concentration of 1% and incubated at 37°C for 10 min. The cells were washed in 1 mL of ice-cold PBS with proteinase inhibitors, scraped, and resuspended in 400 μL of SDS lysis buffer. Lysates were sonicated for 10 s nine times on ice and centrifuged at 15,000 rpm for 10 min at 4°C. Supernatants were

Table 1. Primer sequences and PCR conditions

	Sense primer (5′ → 3′)	Antisense primer (5′ → 3′)	Annealing temperature (°C), PCR cycles	Product size (bp)
MSP primers				
PAN	GGAGGGAAGGAAGGGTAAG	CAACTCAATAAACTCAAACTCCC	54, 40	260
MSP	GGGTTTTGCGAGAGCGCG	GCTAACAAACGCGAACCG	64, 35	169
USP	GGTTTTGTGAGAGTGTGTTTAG	CACTAACAAACACAAACCAAAC	60, 35	169
RT-PCR primers				
RASSF1A	CAGATTGCAAGTTCACCTGCCACTA	GATGAAGCCTGTGTAAGAACCGTCCT	60, 33	242
GAPDH	GAGTCAACGGATTTGGTCGT	TGGAATCATATTGGAACATGTAAA	60, 32	135
ChIP primers				
1	GATCACGGTCCAGCCTCTGC	CTCGAGCCTTCACTTGGGGT	60, 32	109
2	GCTTCAGCAAACCGGACCAGG	CCGGACGGCCACAACGA	60, 32	134
3	TGGGGTGTGAGGAGGGGACGA	AGAGCCGCGCAATGGA	60, 32	124
4	GTTTCCATTGCGCGGCTCT	CTGGCTTTGGGCGCTAGCAAG	60, 32	124
GAPDH	TACTAGCGGTTTTACGGGCG	TCGAACAGGAGGAGCAGAGAGCGA	60, 32	166

DOI:10.1158/1078-0432.CCR-06-2225

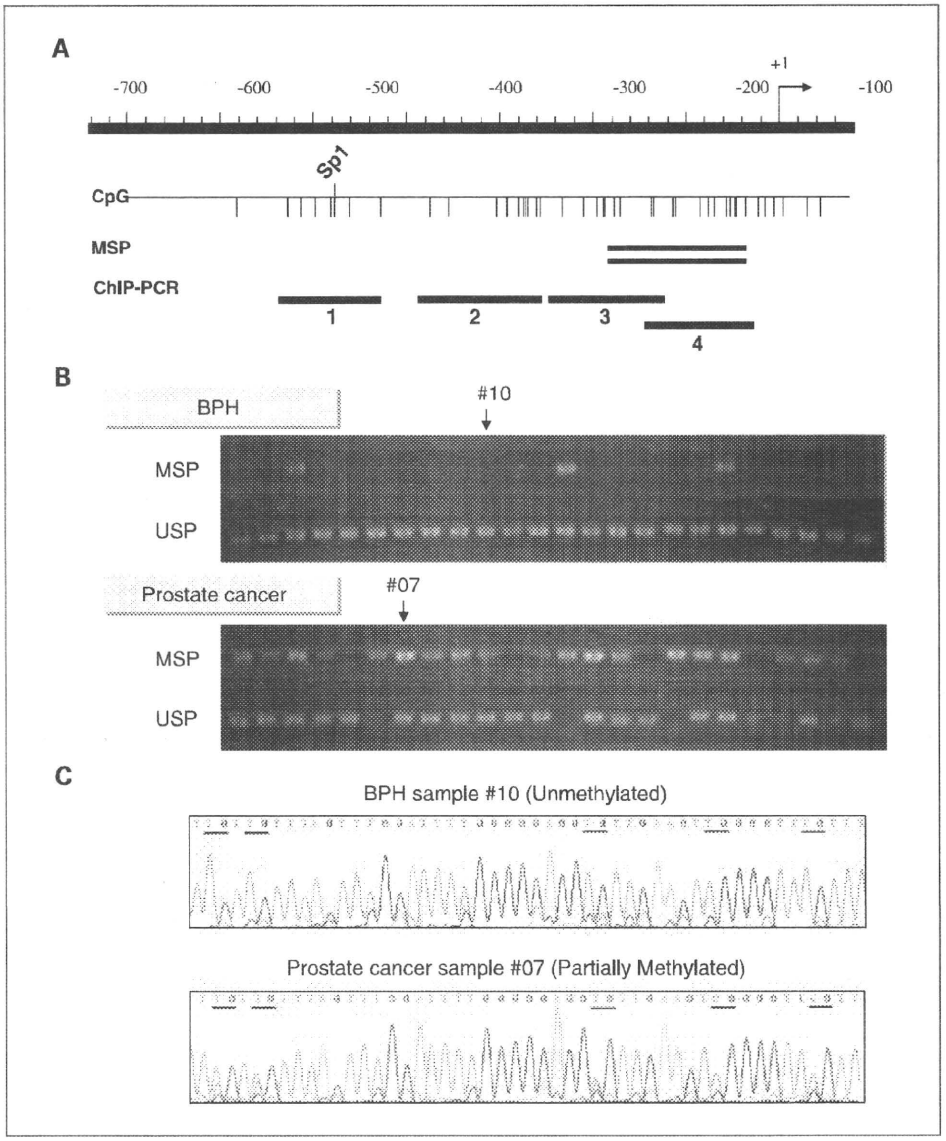

Fig. 1. *A*, schematic representation of the promoter region of the human *RASSF1A* gene. Vertical lines, location of CpG dinucleotides; arrow, approximate position of the transcription start site. Doubled horizontal line, region examined by MSP. Four horizontal bars, location of the DNA fragments amplified by PCR done on the DNA recovered from ChIP assay. *B*, typical MSP results in BPH and prostate cancer samples are shown. Methylated bands were detected in 97 (74.0%) of the prostate cancer samples and in only 12 (18.5%) of the BPH samples. *C*, bisulfite DNA sequencing of unmethylated (*top*) and partially methylated (*bottom*) samples. In unmethylated samples, every CpG site was unmethylated. In partially methylated samples, there was a "T" peak along with a "C" peak at the CpG sites. Bars under the sequence, CpG sites. The results of the bisulfite DNA sequencing were consistent with those obtained by MSP.

loaded on 1% agarose gels and determined to have reduced DNA lengths between 200 and 1,000 bp. The sonicated samples were precleaned with salmon sperm DNA/protein A agarose beads (Upstate Biotechnology). The soluble chromatin fraction was collected, and 8 μL of antibody for acetyl-H3, acetyl-H4, dimethyl-H3-K4 (H3K4me2), or 12 μL of antibody for dimethyl-H3-K9 (H3K9me2), or no antibody, was added and incubated overnight with rotation (23). All antibodies were purchased from Upstate Biotechnology. After rotation, chromatin-antibody complexes were collected using salmon sperm DNA/protein A agarose beads and washed according to the manufacturer's protocol. Immunoprecipitated DNA was recovered using a QIAquick PCR Purification Kit (Qiagen) and analyzed by PCR. We used previously reported (23, 24) primers designed to separately amplify four regions in the *RASSF1A* promoter area (Fig. 1A). The primer pairs used for ChIP assays are shown in Table 1. One additional primer set was used to amplify a 166-bp fragment of the glyceraldehyde-3-phosphate dehydrogenase (*GAPDH*) gene as an internal control. Each PCR reaction was initially set up using different amounts of ChIP sample with varying PCR cycle numbers, and we selected the final PCR conditions accordingly. PCR products were analyzed on 3.0% agarose gels and visualized by UV illumination. Densitometric analysis of the observed bands was done using ImageJ software.[4] Relative enrichment was calculated by taking the ratio between the net intensity of the *RASSF1A* PCR product from each primer set and the net intensity of the *GAPDH* PCR product for the bound sample and dividing this by the same ratio calculated for the input sample (25). The value of each point was calculated as the average from two independent ChIP experiments and a total of four independent PCR analyses.

Statistical analysis. The relationship between clinicopathologic findings and methylation status of the *RASSF1A* gene was done using the χ^2 test and Fisher's exact test. For each clinicopathologic finding, the association with PSA failure-free probability was determined using Kaplan-Meier curves, and a log-rank test was used to determine significance. *P* values of <0.05 were regarded as statistically significant. All statistical analyses were done using StatView version 5.0 for Windows.

[4] http://rsb.info.nih.gov/ij

DOI:10.1158/1078-0432.CCR-06-2225

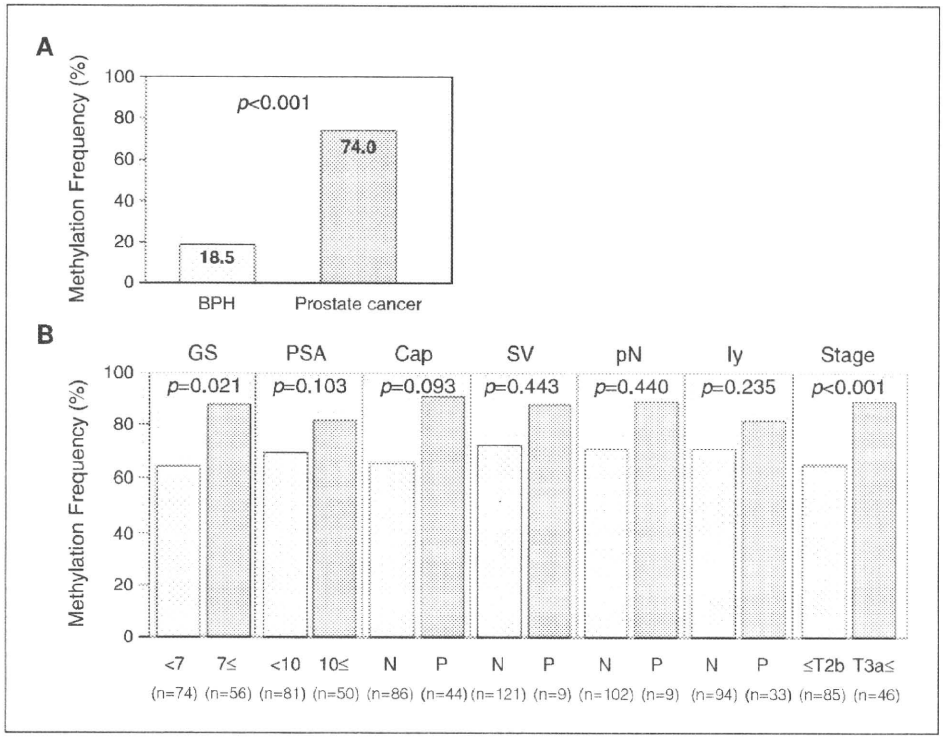

Fig. 2. Correlation of clinicopathologic features with methylation frequency of the *RASSF1A* promoter. *A*, the difference in the frequency of *RASSF1A* promoter methylation was significant between prostate cancer and BPH samples. *B*, there was significant correlation between methylation frequency of *RASSF1A* and high GS or clinical stage. Methylation frequency of *RASSF1A* increased with higher GS and high stage. The total number of patients was 131, but some patients were lacking clinicopathologic findings, and then data were not included. Cap, capsular invasion; SV, seminal vesicle involvement; pN, lymph node invasion; Iy, lymphatic vessel invasion. N and P, negative and positive, respectively.

Results

Methylation status of RASSF1A gene. Typical examples of MSP and USP bands obtained during methylation analysis of the *RASSF1A* promoter are shown in Fig. 1B. To confirm the methylation status of the *RASSF1A* promoter, bisulfite-modified DNA was amplified and sequenced. Typical bisulfite-modified DNA sequencing of prostate cancer and BPH samples are shown in Fig. 1C. In BPH samples, most CpG sites were not methylated, whereas in prostate cancer samples, most CpG sites were methylated in the promoter region. In the total group of prostate cancer and BPH, there was no correlation between age and methylation. In the 131 prostate cancer samples, positive *RASSF1A* methylation was detected in 97

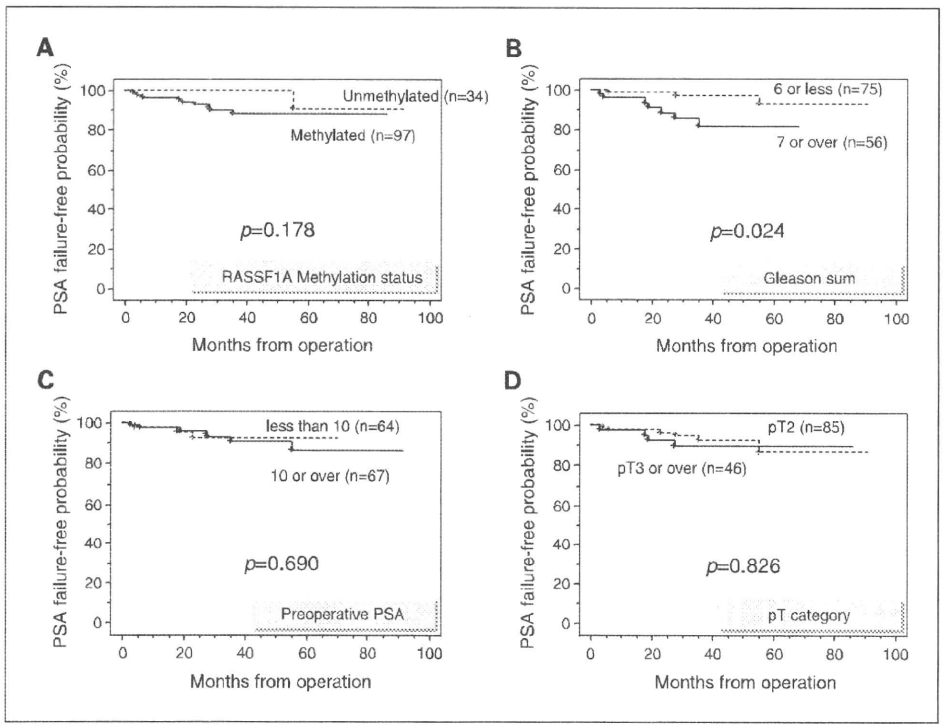

Fig. 3. Kaplan-Meier PSA failure-free survival curves of prostate cancer patients after radical prostatectomy, grouped according to the evaluated variables. *A*, methylation frequency of *RASSF1A*; *B*, GS; *C*, preoperative PSA; *D*, pT category. Follow-up ranged from 0.7 to 91.4 mo, with a median of 35.5 mo.

DOI:10.1158/1078-0432.CCR-06-2225

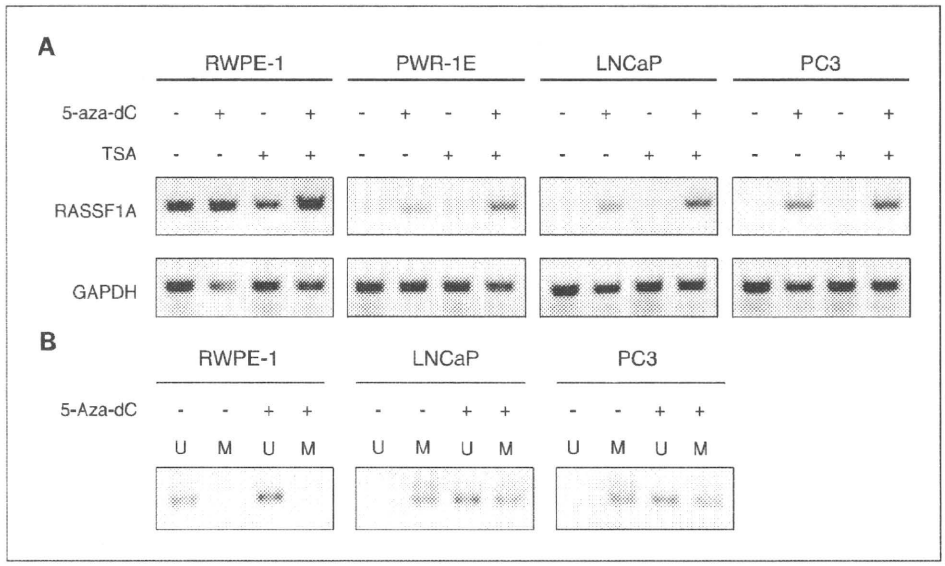

Fig. 4. *A*, RT-PCR analysis of *RASSF1A* expression in a normal prostatic epithelial cell lines and two prostate cancer cell lines. The mRNA transcript of *RASSF1A* was significantly increased after 5-aza-dC treatment alone or with a combination of 5-aza-dC and TSA in PWR-1E and the two cancer cell lines. In contrast, TSA treatment failed to re-express the *RASSF1A* gene in these cell lines. *GAPDH* expression served as a loading control. *B*, MSP analysis of *RASSF1A*. MSP analysis showed partial demethylation of the *RASSF1A* promoter region after 5-aza-dC treatment in prostate cancer cell lines. M, reactions specific for methylated DNA; U, reactions specific for unmethylated DNA.

samples (74.0%). On the other hand, in 65 BPH samples, positive *RASSF1A* methylation was detected in 12 samples (18.5%). The difference in the frequency of *RASSF1A* promoter methylation was significant between prostate cancer and BPH samples ($P < 0.001$; Fig. 2A). The methylation frequency of *RASSF1A* showed a significant increase with high GS (63% in GS <7, and 88% in GS ≥7; $P = 0.002$; Fig. 2B) and clinical stage (65% in stage ≤T2b and 91% in stage ≥T3a; $P < 0.001$; Fig. 2B). Although there was a tendency toward increased *RASSF1A* promoter methylation, there was no significant association with high PSA or other pathologic categories (Fig. 2B). PSA failure-free probability was analyzed as disease-free survival, with PSA failure occurring in 10 patients (7.6%). Of the clinicopathologic features considered, only GS was significantly associated with poor outcome ($P = 0.022$; Fig. 3B).

Effects of 5-aza-dC and TSA on RASSF1A gene expression in prostate cancer cells. To clarify the role of epigenetic suppression of the *RASSF1A* gene, we treated prostate cancer cell lines with 5-aza-dC and TSA. At baseline, expression of the *RASSF1A* mRNA transcript was detected in the normal prostate cell line (RWPE-1), but was negative in PWR-1E and prostate cancer cell lines (LNCaP and PC3). With TSA treatment, *RASSF1A* re-expression was not detected in prostate cancer cell lines. However, the expression level was significantly increased in both prostate cancer cell lines after treatment with the demethylating agent 5-aza-dC or combined treatment with azaC and TSA (Fig. 4A). To determine the effects of the demethylating agent, we examined the methylation status in LNCaP and PC3 cells after 5-aza-dC treatment. In both cell lines, partial demethylation was detected by MSP (Fig. 4B).

ChIP assay. The association of *RASSF1A* promoter methylation and gene silencing in relation to chromatin remodeling has not been reported previously in prostate cancer. To establish this functional link, we examined local histone acetylation and H3 methylation in the chromatin associated with the *RASSF1A* promoter region using a ChIP assay. The histone-associated DNAs, immunoprecipitated with antibodies against acetyl-H3, acetyl-H4, H3K4me2, or H3K9me2, were individually amplified with four primer sets covering the *RASSF1A* promoter region (Fig. 1A). The results in Fig. 5 show marked differences in the levels of histone acetylation and H3 methylation. Enhancement of histone acetylation and H3K4me2 methylation was observed in RWPE-1 cells, in which the *RASSF1A* promoter is unmethylated and transcriptionally active; however, there was no acetylation or methylation of these same sites in the hypermethylated, transcriptionally silenced promoters (PWR-1E, LNCaP, and PC3). In contrast, H3K9me2 was enriched along the entire hypermethylated and transcriptionally inactive promoters.

To investigate the effect of DNA methyltransferase inhibitor and HDAC-I in the histone modifications of *RASSF1A* promoter, we treated LNCaP cells with 5-aza-dC and/or TSA (Fig. 6A and B). The ChIP assays revealed that TSA treatment alone did not induce any alteration of histone modification. These data show that in addition to being unable to reactivate expression of a hypermethylated, silenced *RASSF1A* gene, TSA alone was unable to evoke obvious change in key parameters of the histone code in the *RASSF1A* promoter (25). In contrast, we observed a complete reversal of the histone modifications after 5-aza-dC treatment alone or the combination of 5-aza-dC and TSA. Acetyl-H3, acetyl-H4, and H3K4me2 levels were higher, whereas H3K9me2 levels were lower in the promoter region.

Discussion

Transcriptional gene silencing by hypermethylation of CpG islands in the promoter region is becoming recognized as a common mechanism for the inactivation of tumor suppressor genes in human malignancies (26–28). In recent years, the list of tumor suppressor genes that are inactivated by epigenetic events rather than classic mutation/deletion events has been growing (7). Unlike mutational inactivation, methylation is reversible, and demethylating agents and inhibitors of HDACs are being used in clinical trails (7).

DNA methylation is an important mechanism in prostate cancer and is involved in the inactivation of various essential genes such as E-cadherin (29), MDR1 (30), and glutathione *S*-transferase P1 (31). In this study, we found that the *RASSF1A*

DOI:10.1158/1078-0432.CCR-06-2225

gene was methylated in 74% of prostate cancer cases examined. Liu et al. (15) has also reported that *RASSF1A* methylation was frequently observed in prostate cancer (71%). *RASSF1A* functions as a tumor suppressor gene through several distinct pathways, including microtubule stability (32, 33) and cell cycle regulation (8, 16, 34). The *RASSF1A* gene has several isoforms, including *RASSF1A* and *RASSF1C* that are transcribed from two different promoters containing CpG islands (10, 11). Selective promoter methylation of the *RASSF1A* promoter, but not RASSF1C, is frequent in many cancers, including lung, breast, ovarian, and renal cell carcinomas (10–13). In prostate cancer, inactivation of the *RASSF1A* gene was reported to be related to carcinogenesis, and Maruyama et al. (3) described a significant correlation between methylation status, GS, PSA levels, and stage. The results of the present study also showed that *RASSF1A* promoter methylation was associated with high GS and clinical stage. Currently, Rosenbaum et al. (35) reported that the methylation status of selected genes (GSTPI, APC) in prostate cancer specimens may be predictive for time to recurrence in patients undergoing prostatectomy. We also analyzed PSA failure-free probability as disease-free survival. Of the clinicopathologic features considered, only GS was significantly associated with poor outcome.

The mechanisms of *RASSF1A* epigenetic change in relation to prostate tumorigenesis, especially chromatin structural changes during the silencing of the genes, are not known. Thus, we examined the molecular mechanisms of inactivation of the *RASSF1A* gene by analysis of chromatin remodeling such as CpG methylation in the promoter regions, histone acetylation (acetyl-H3, acetyl-H4), dimethyl-H3-K4 (H3K4me2) and dimethyl-H3-K9 (H3K9me2) methylation associated with the *RASSF1A* promoter region. Histone acetylation and H3K4me2 methylation were increased in the unmethylated RWPE-1 *RASSF1A* promoter; however, there was no acetylation or methylation of these same sites in the hypermethylated LNCaP and PC3 promoter. In contrast, H3K9me2 was enriched along the entire hypermethylated and transcriptionally inactive promoter in LNCaP and PC3 cells. Similar results has been reported in breast cancer (23, 24). These results support the idea that DNA methylation-mediated gene silencing is closely linked with repressive histone modifications at the gene promoter in cancer cells (23, 25, 36).

In this study, we also investigated the effect of a DNA methyltransferase inhibitor (5-aza-dC) and/or a HDAC-inhibitor (TSA) on chromatin remodeling. We treated LNCaP cells with TSA alone, but there was no change in histone acetylation and H3

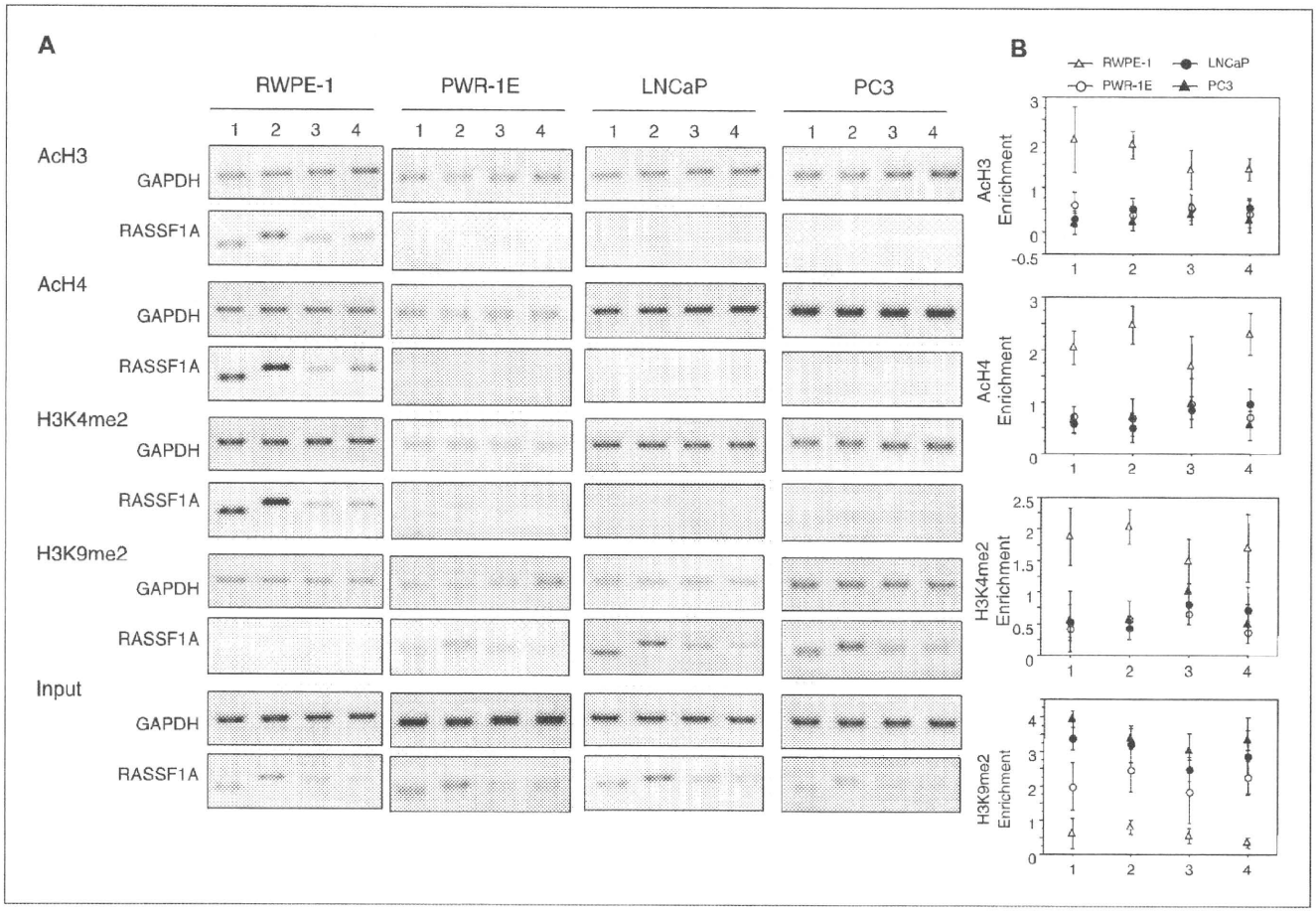

Fig. 5. ChIP assays of the *RASSF1A* CpG island. Chromatin DNA was immunoprecipitated with antibodies specific for acetyl-H3, acetyl-H4, dimethyl-H3-K4 (H3K4me2), and dimethyl-H3-K9 (H3K9me2), respectively. DNA fragments corresponding to *RASSF1A* promoter regions 1, 2, 3, and 4 (see Fig. 1A) were amplified by PCR. Enhancement of histone acetylation and H3K4me2 methylation was observed in the RWPE-1 promoter. However, there was no acetylation or methylation of these same sites in PWR-1E, LNCaP, and PC3 cells. In contrast, H3K9me2 was enriched in these cell lines. *A*, PCR analyses of ChIP assay on RWPE-1, PWR-1E, LNCaP, and PC3 cells in the four promoter regions. *B*, points, enrichment data calculated from the corresponding DNA fragments amplified by PCR; bars SD.

DOI:10.1158/1078-0432.CCR-06-2225

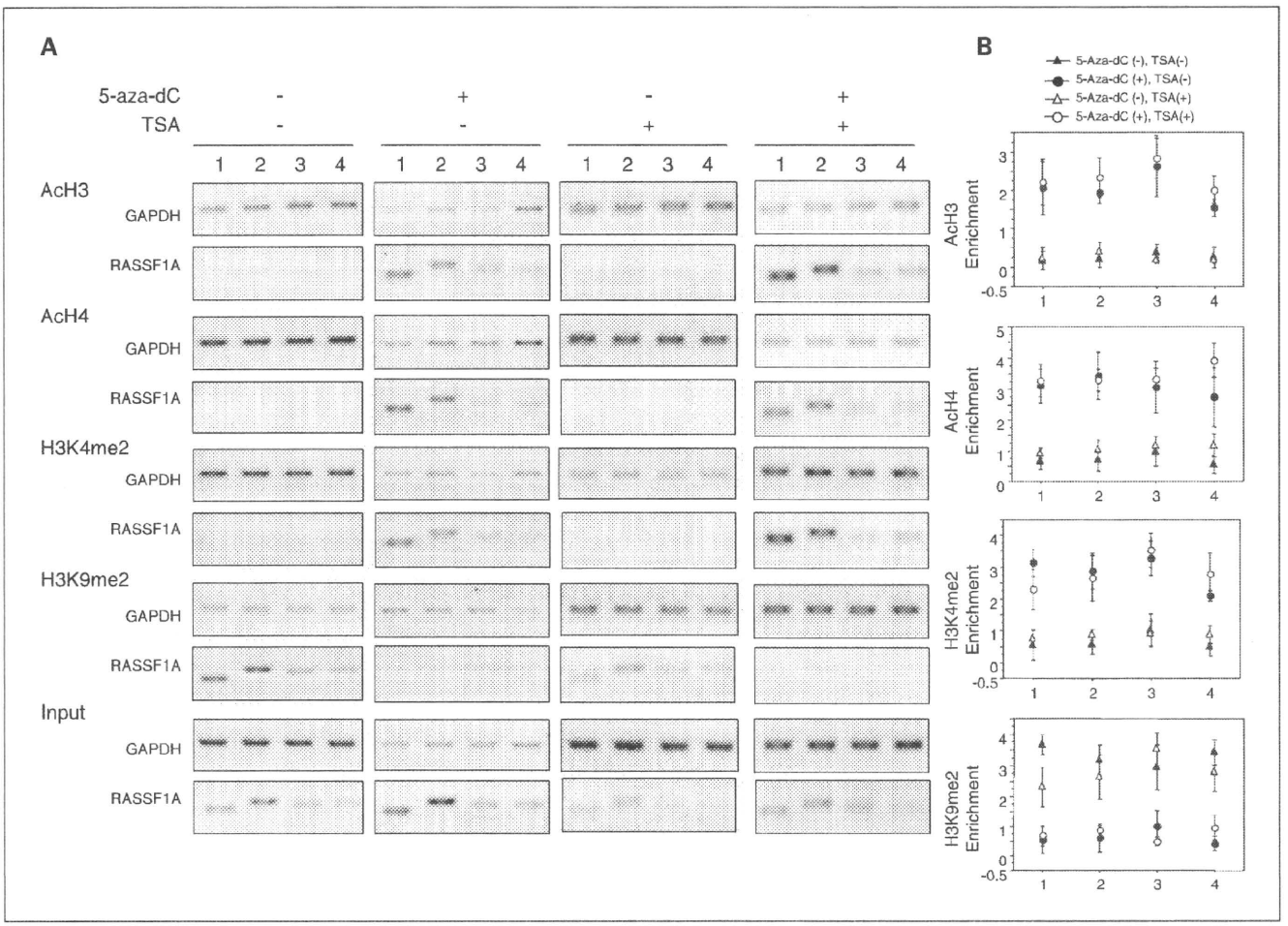

Fig. 6. Effects of 5-aza-dC and TSA on the histone modifications of the *RASSF1A* promoter. ChIP assays were done on LNCaP calls after treatment with 5 μmol/L 5-aza-dC for 48 h and/or 300 nmol/L TSA for 24 h. TSA treatment alone did not induce any alteration of histone modification. In contrast, complete reversal of the histone modifications were observed after 5-aza-dC treatment alone or the combination of 5-aza-dC and TSA. Acetyl-H3, acetyl-H4, and H3K4me2 levels were higher, whereas H3K9me2 levels were lower in this region of the promoter. *A*, PCR analyses of ChIP assays. *B*, points, enrichment data calculated from the corresponding DNA fragments amplified by PCR; bars, SD.

methylation. In contrast, after 5-aza-dC treatment alone or a combination of 5-aza-dC and TSA, there was increased accumulation of acetylated histones and H3K4me2 methylation concomitant with reactivation of the methylated *RASSF1A* promoter. These results favor the idea that DNA methylation is more important compared with histone deacetylation in maintaining a silent state at hypermethylated promoters because 5-aza-dC can reactivate genes silenced with aberrant promoter hypermethylation, but TSA alone did not reactivate these genes (37). This change in histone modification upon inhibition of DNA methyltransferase suggests that in prostate cancer cells, DNA hypermethylation, or another activity mediated by DNA methyltransferase, may also be essential for maintaining repressive histone modifications at gene promoters silenced by aberrant DNA hypermethylation (25). Furthermore, the observation that 5-aza-dC can both reactivate expression of the silenced *RASSF1A* gene and completely reverse key histone modifications surrounding the gene promoter strengthens the idea that interdependence exists between these two events.

In conclusion, this is the first report suggesting that chromatin remodeling, such as reduced histone acetylation and H3K4me2 methylation, and increased H3K9me2 methylation play a critical role in the maintenance of promoter DNA methylation-associated gene silencing in prostate cancer.

References

1. Jemal A, Ward E, Hao Y, Thun M. Trends in the leading causes of death in the United States, 1970–2002. JAMA 2005;294:1255–9.
2. Perry AS, Foley R, Woodson K, Lawler M. The emerging roles of DNA methylation in the clinical management of prostate cancer. Endocr Relat Cancer 2006; 13:357–77.
3. Maruyama R, Toyooka S, Toyooka KO, et al. Aberrant promoter methylation profile of prostate cancers and its relationship to clinicopathological features. Clin Cancer Res 2002;8:514–9.
4. Esteller M. CpG island hypermethylation and tumor suppressor genes: a booming present, a brighter future. Oncogene 2002;21:5427–40.
5. Jeronimo C, Henrique R, Hoque MO, et al. A quantitative promoter methylation profile of prostate cancer. Clin Cancer Res 2004;10:8472–8.
6. Sidransky D. Emerging molecular markers of cancer. Nat Rev Cancer 2002;2:210–9.
7. Agathanggelou A, Cooper WN, Latif F. Role of the Ras-association domain family 1 tumor

DOI:10.1158/1078-0432.CCR-06-2225

suppressor gene in human cancers. Cancer Res 2005; 65:3497–508.
8. Pfeifer GP, Dammann R. Methylation of the tumor suppressor gene RASSF1A in human tumors. Biochemistry (Mosc) 2005;70:576–83.
9. Liu L, Broaddus RR, Yao JC, et al. Epigenetic alterations in neuroendocrine tumors: methylation of RAS-association domain family 1, isoform A and p16 genes are associated with metastasis. Mod Pathol 2005;18: 1632–40.
10. Burbee DG, Forgacs E, Zochbauer-Muller S, et al. Epigenetic inactivation of RASSF1A in lung and breast cancers and malignant phenotype suppression. J Natl Cancer Inst 2001;93:691–9.
11. Dammann R, Li C, Yoon JH, Chin PL, Bates S, Pfeifer GP. Epigenetic inactivation of a RAS association domain family protein from the lung tumour suppressor locus 3p21.3. Nat Genet 2000;25:315–9.
12. Agathanggelou A, Honorio S, Macartney DP, et al. Methylation associated inactivation of RASSF1A from region 3p21.3 in lung, breast and ovarian tumours. Oncogene 2001;20:1509–18.
13. Dreijerink K, Braga E, Kuzmin I, et al. The candidate tumor suppressor gene, RASSF1A, from human chromosome 3p21.3 is involved in kidney tumorigenesis. Proc Natl Acad Sci U S A 2001;98:7504–9.
14. Yegnasubramanian S, Kowalski J, Gonzalgo ML, et al. Hypermethylation of CpG islands in primary and metastatic human prostate cancer. Cancer Res 2004; 64:1975–86.
15. Liu L, Yoon JH, Dammann R, Pfeifer GP. Frequent hypermethylation of the RASSF1A gene in prostate cancer. Oncogene 2002;21:6835–40.
16. Dammann R, Schagdarsurengin U, Seidel C, et al. The tumor suppressor RASSF1A in human carcinogenesis: an update. Histol Histopathol 2005;20: 645–63.
17. Bastian PJ, Ellinger J, Wellmann A, et al. Diagnostic and prognostic information in prostate cancer with the help of a small set of hypermethylated gene loci. Clin Cancer Res 2005;11:4097–106.
18. The Japanese Urological Association and Japanese Society of Pathology. General rules for clinical and pathological studies on prostate cancer. 2nd ed. Tokyo (Japan): Kanahara-shuppan Co.; 1992.
19. Shigeno K, Igawa M, Shiina H, Kishi H, Urakami S. Transrectal colour Doppler ultrasonography for quantifying angiogenesis in prostate cancer. BJU Int 2003; 91:223–6.
20. Dahiya R, Lee C, McCarville J, Hu W, Kaur G, Deng G. High frequency of genetic instability of microsatellites in human prostatic adenocarcinoma. Int J Cancer 1997;72:762–7.
21. Herman JG, Graff JR, Myohanen S, Nelkin BD, Baylin SB. Methylation-specific PCR: a novel PCR assay for methylation status of CpG islands. Proc Natl Acad Sci U S A 1996;93:9821–6.
22. Lo KW, Kwong J, Hui AB, et al. High frequency of promoter hypermethylation of RASSF1A in nasopharyngeal carcinoma. Cancer Res 2001;61:3877–81.
23. Yan PS, Shi H, Rahmatpanah F, et al. Differential distribution of DNA methylation within the RASSF1A CpG island in breast cancer. Cancer Res 2003;63: 6178–86.
24. Strunnikova M, Schagdarsurengin U, Kehlen A, Garbe JC, Stampfer MR, Dammann R. Chromatin inactivation precedes *de novo* DNA methylation during the progressive epigenetic silencing of the RASSF1A promoter. Mol Cell Biol 2005;25:3923–33.
25. Fahrner JA, Eguchi S, Herman JG, Baylin SB. Dependence of histone modifications and gene expression on DNA hypermethylation in cancer. Cancer Res 2002;62:7213–8.
26. Jones PA, Laird PW. Cancer epigenetics comes of age. Nat Genet 1999;21:163–7.
27. Baylin SB, Herman JG. DNA hypermethylation in tumorigenesis: epigenetics joins genetics. Trends Genet 2000;16:168–74.
28. Kawaguchi K, Oda Y, Saito T, et al. DNA hypermethylation status of multiple genes in soft tissue sarcomas. Mod Pathol 2006;19:106–14.
29. Li LC, Zhao H, Nakajima K, et al. Methylation of the E-cadherin gene promoter correlates with progression of prostate cancer. J Urol 2001;166:705–9.
30. Enokida H, Shiina H, Igawa M, et al. CpG hypermethylation of MDR1 gene contributes to the pathogenesis and progression of human prostate cancer. Cancer Res 2004;64:5956–62.
31. Enokida H, Shiina H, Urakami S, et al. Ethnic group-related differences in CpG hypermethylation of the GSTP1 gene promoter among African-American, Caucasian and Asian patients with prostate cancer. Int J Cancer 2005;116:174–81.
32. Mathe E. RASSF1A, the new guardian of mitosis. Nat Genet 2004;36:117–8.
33. Jackson PK. Linking tumor suppression, DNA damage and the anaphase-promoting complex. Trends Cell Biol 2004;14:331–4.
34. Shivakumar L, Minna J, Sakamaki T, Pestell R, White MA. The RASSF1A tumor suppressor blocks cell cycle progression and inhibits cyclin D1 accumulation. Mol Cell Biol 2002;22:4309–18.
35. Rosenbaum E, Hoque MO, Cohen Y, et al. Promoter hypermethylation as an independent prognostic factor for relapse in patients with prostate cancer following radical prostatectomy. Clin Cancer Res 2005;11: 8321–5.
36. Jones PA, Baylin SB. The fundamental role of epigenetic events in cancer. Nat Rev Genet 2002;3: 415–28.
37. Cameron EE, Bachman KE, Myohanen S, Herman JG, Baylin SB. Synergy of demethylation and histone deacetylase inhibition in the re-expression of genes silenced in cancer. Nat Genet 1999;21:103–7.